

# Supplementary Material: A Study of the Trade-off between Reducing Precision and Reducing Resolution for Data Analysis and Visualization

Table 1: All data sets used in experiments. The resolution of data sets is  $64^3$  and they are subsets of the original volumes (no downsampling performed).

Name	Type	Data type
boiler [9]	combustion simulation	float64
plasma [4]	magnetic reconnection simulation	float32
diffusivity [1]	hydrodynamics simulation	float64
pressure [1]	hydrodynamics simulation	float64
turbulence [2]	fluid dynamics simulation	float32
kingsnake [3]	scan of a snake egg	uint8
flame [5]	combustion simulation	float32
csafe	fluid dynamics simulation	uint8
enzo v [7]	cosmology simulation	float32
brain	microscope image of a marmoset brain	uint8
foam [6]	CT scan of an aluminum foam	uint16
vismale	CT scan of a human	uint8
karfs [8]	combustion simulation	float32
aneurysm	scan of brain aneurysm	uint8
velocity z [1]	hydrodynamics simulation	float64

## 1 Acknowledgement

We thank all the researchers who kindly shared with us their data sets to use for experiments in this paper. In particular, Benjamin Isaac provides the *boiler* and Kristoffer Matheson and Ashley Spear provides the *foam* data sets. Hong Im and Paul Arias provide *flame* [5]. The *karfs* [8] data set is kindly shared with us by Hong Im, Francisco Hernandez Perez, Ramanan Sankaran and Bok Jik Lee. We also thank Frederick Federer and Alessandra Angelucci for the *brain* data set. *csafe* is courtesy of the Center for the Simulation of Accidental Fires and Explosions (CSAFE) at the Scientific Computing and Imaging Institute (SCI), University of Utah. *vismale* is courtesy of the U.S. National Library of Medicine. Finally, the *aneurysm* data set is courtesy of Philips Research, Hamburg, Germany.

## References

- [1] A. W. Cook, W. Cabot, and P. L. Miller. The mixing transition in Rayleigh-Taylor instability. *Journal of Fluid Mechanics*, 511:333–362, 2004.
- [2] D. A. Donzis, P. Yeung, and D. Pekurovsky. Turbulence simulations on  $\mathcal{O}(10^4)$  processors. In *TeraGrid*, 2008.
- [3] A. Gosselin-Ildari. The deep scaly project, "lampropeltis getula" (on-line), digital morphology. [http://digimorph.org/specimens/Lampropeltis\\_getula/adult/](http://digimorph.org/specimens/Lampropeltis_getula/adult/) (accessed on July 23, 2018), 2006.
- [4] F. Guo, H. Li, W. Daughton, and Y.-H. Liu. Formation of hard power-laws in the energetic particle spectra resulting from relativistic magnetic reconnection. *Physical Review Letters*, 113, 2014.
- [5] H. G. Im, P. G. Arias, S. Chaudhuri, and H. A. Uranakara. Direct numerical simulations of statistically stationary turbulent premixed flames. *Combustion Science and Technology*, 188(8):1182–1198, 2016.
- [6] K. E. Matheson, K. K. Cross, M. M. Nowell, and A. D. Spear. A multiscale comparison of stochastic open-cell aluminum foam produced via conventional and additive-manufacturing routes. *Materials Science and Engineering: A*, 707:181–192, 2017.
- [7] B. W. O’shea, G. Bryan, J. Bordner, M. L. Norman, T. Abel, R. Harkness, and A. Kritsuk. Introducing enzo, an amr cosmology application. In *Adaptive Mesh Refinement - Theory and Applications*, pp. 341–349. Springer Berlin Heidelberg, 2005.
- [8] F. E. H. Prez, N. Mukhadiyev, X. Xu, A. Sow, B. J. Lee, R. Sankaran, and H. G. Im. Direct numerical simulations of reacting flows with detailed chemistry using many-core/gpu acceleration. *Computers & Fluids*, 2018.
- [9] P. Smith, J. Thornock, Y. Wu, S. Smith, and B. Isaac. Oxy-coal power boiler simulation and validation through extreme computing. In *International Conference on Numerical Combustion*, 2015.

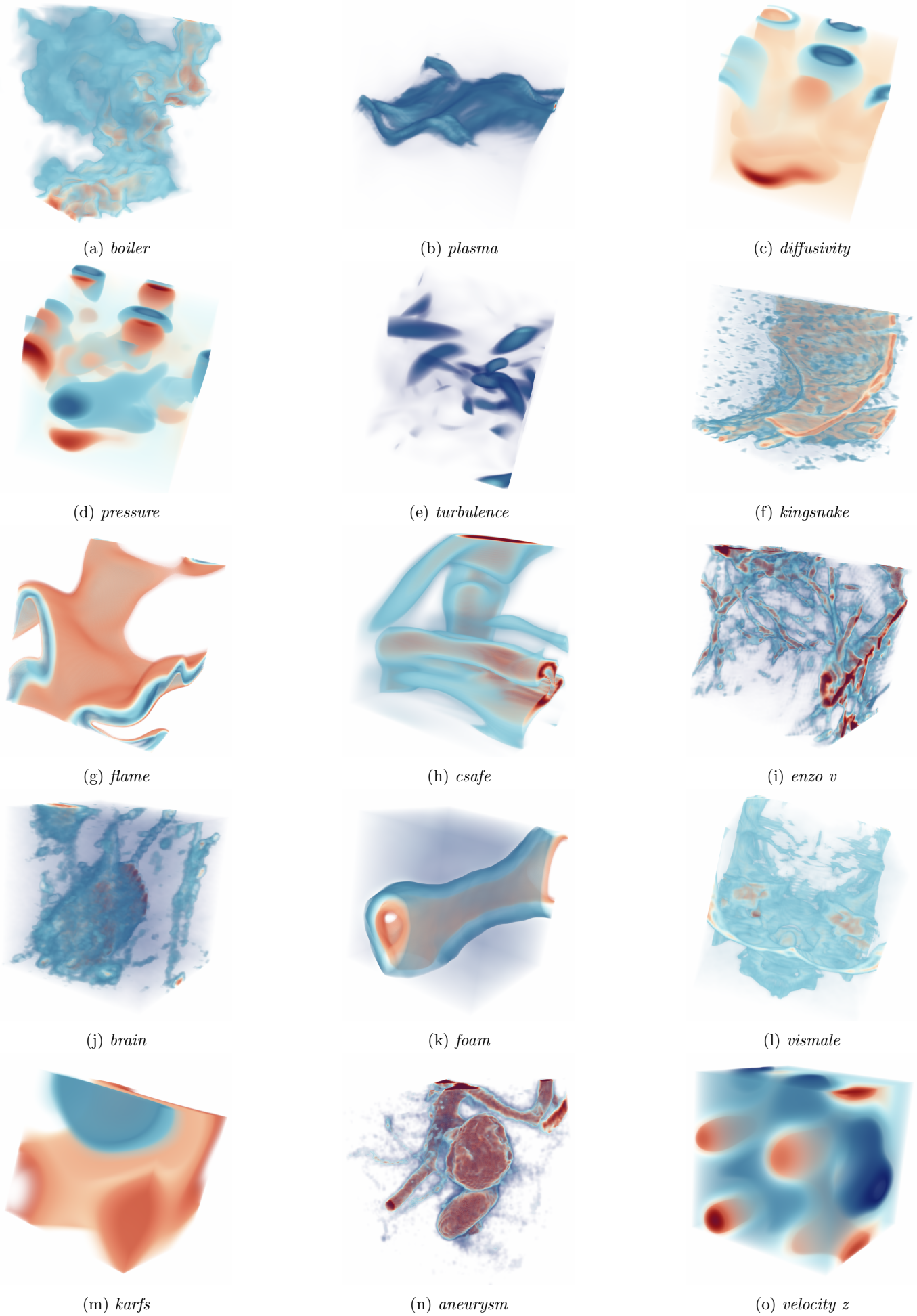
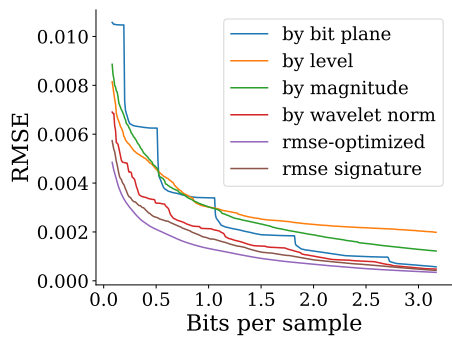
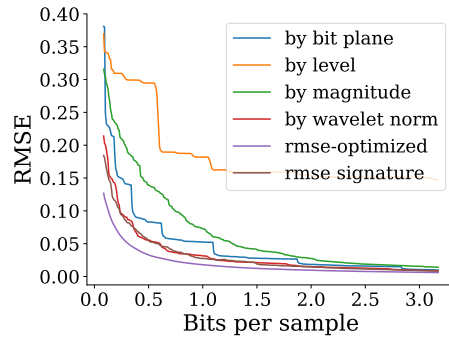


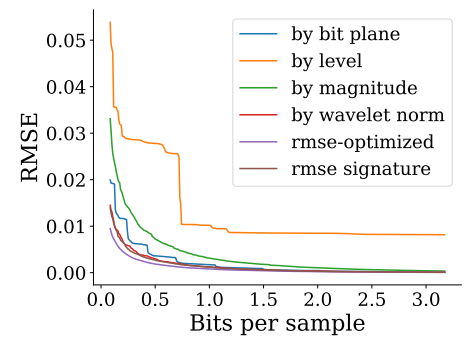
Figure 1: Volume renderings of all data sets



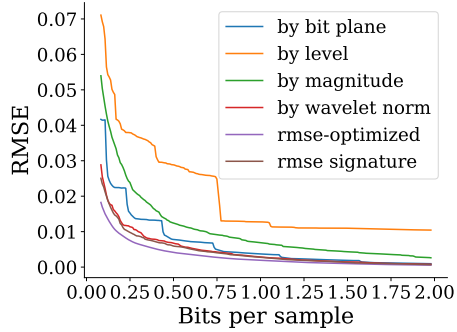
(a) boiler



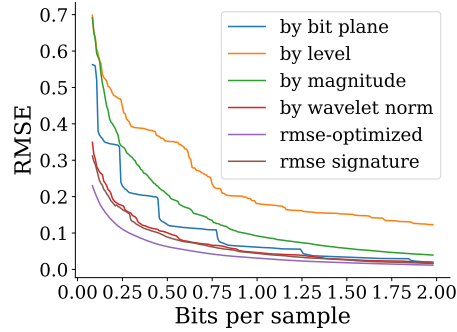
(b) plasma



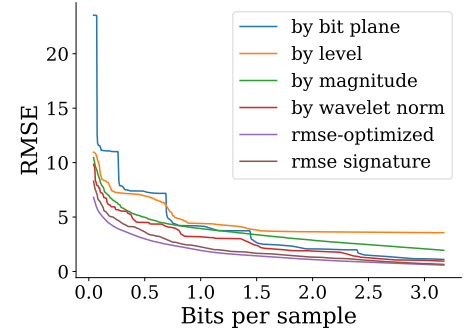
(c) diffusivity



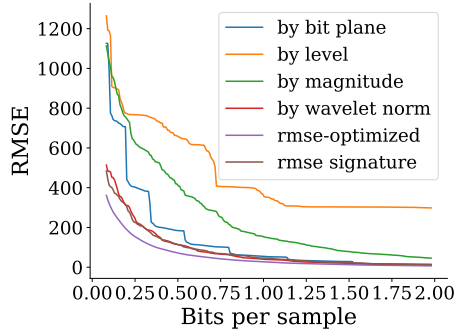
(d) pressure



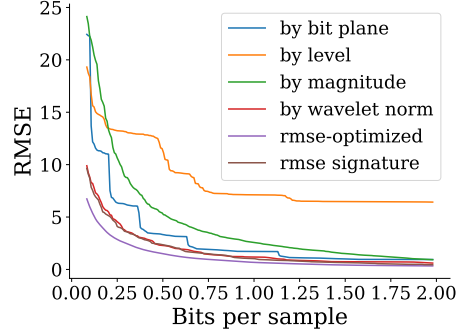
(e) turbulence



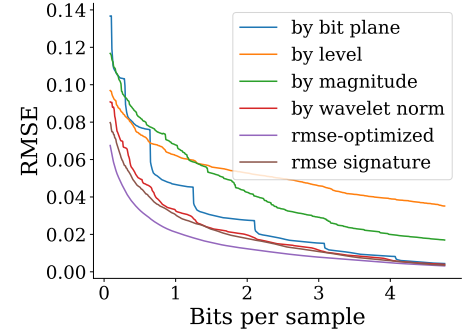
(f) kingsnake



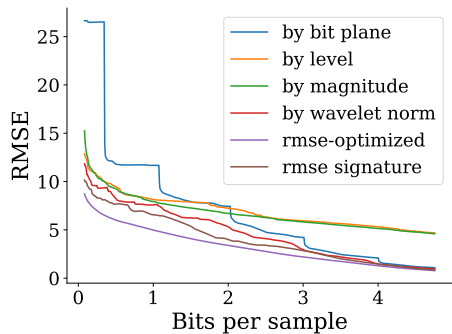
(g) flame



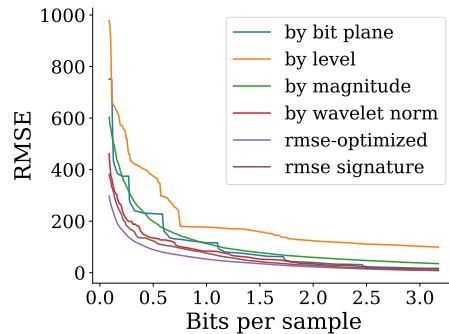
(h) csafe



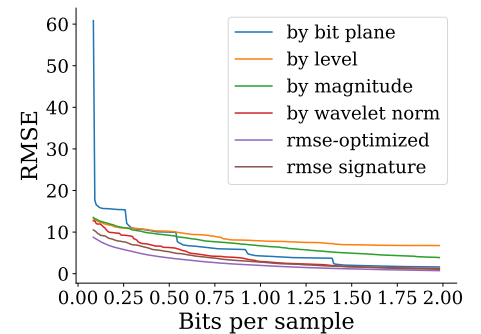
(i) enzo v



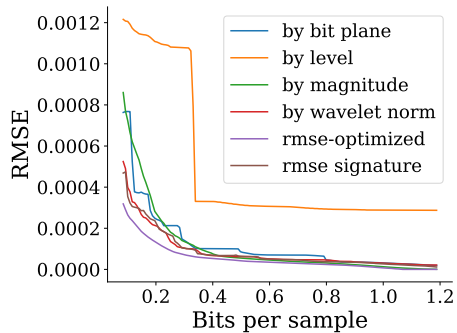
(j) brain



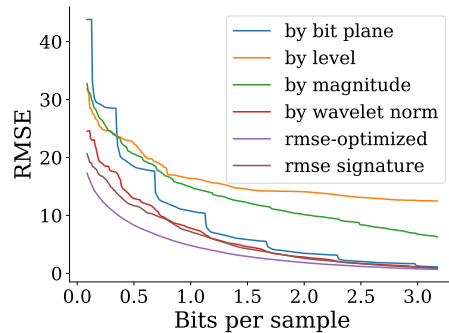
(k) foam



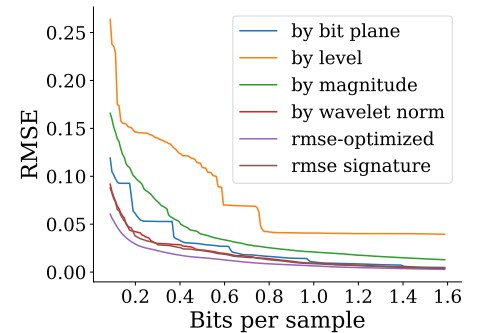
(l) vismale



(m) karfs

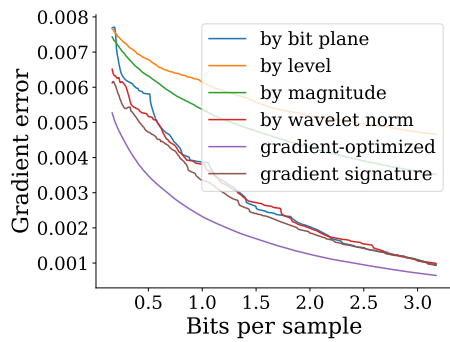


(n) aneurysm

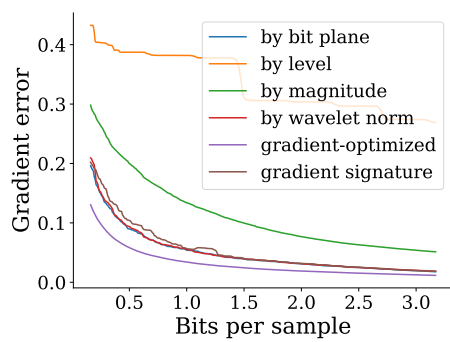


(o) velocity z

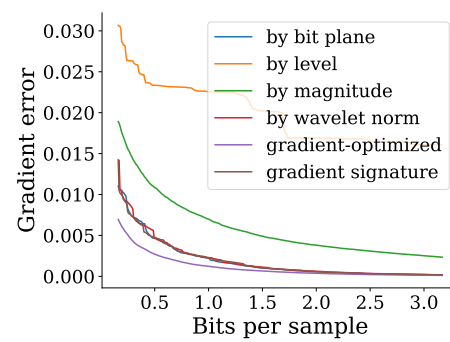
Figure 2: RMSE



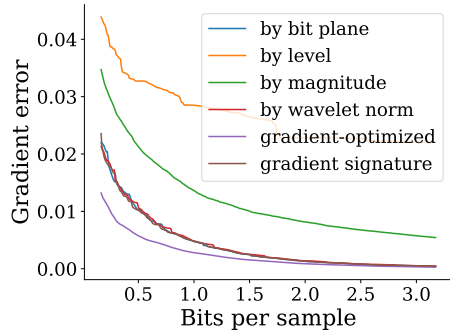
(a) boiler



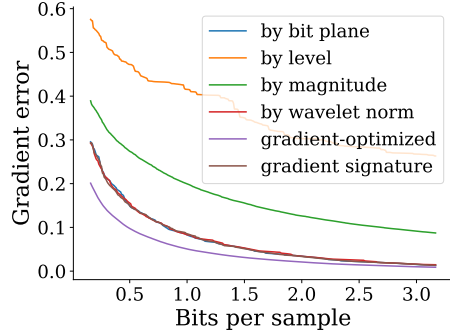
(b) plasma



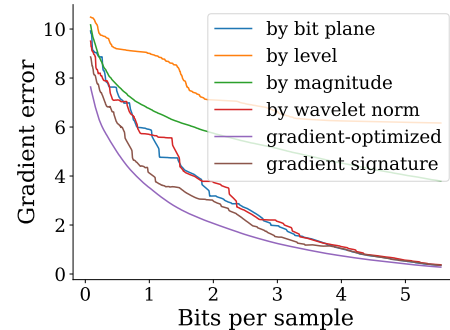
(c) diffusivity



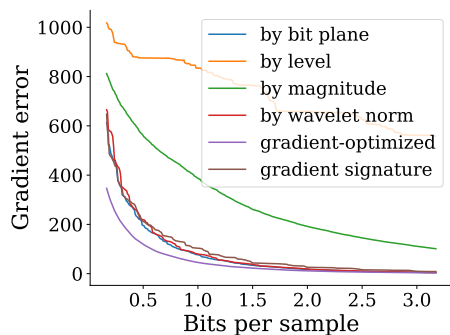
(d) pressure



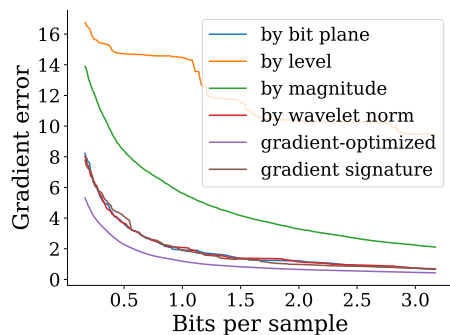
(e) turbulence



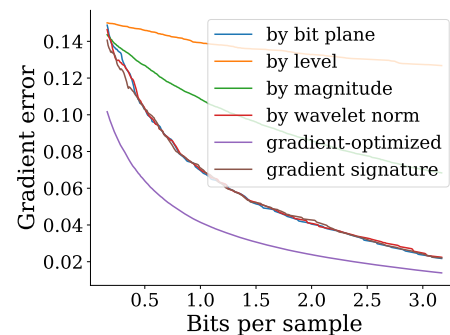
(f) kingsnake



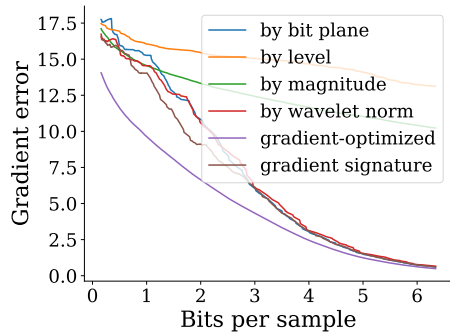
(g) flame



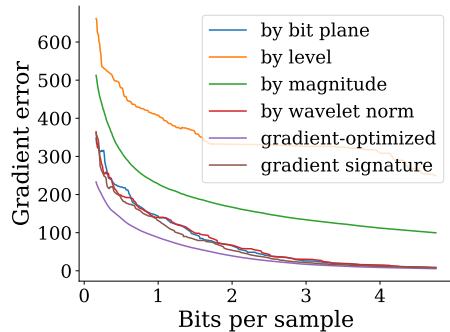
(h) csafe



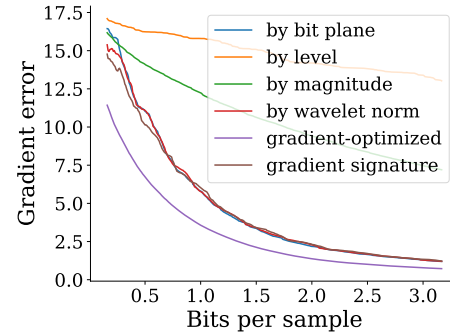
(i) enzo v



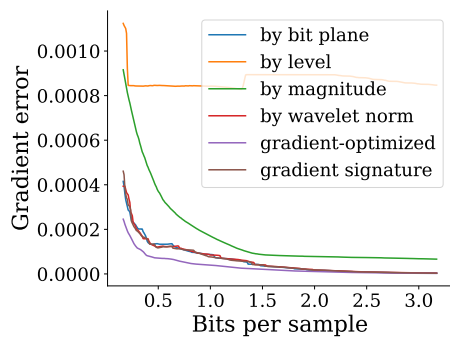
(j) brain



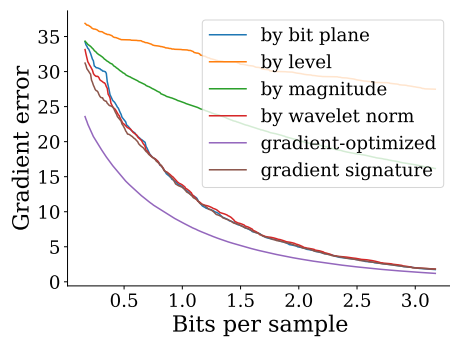
(k) foam



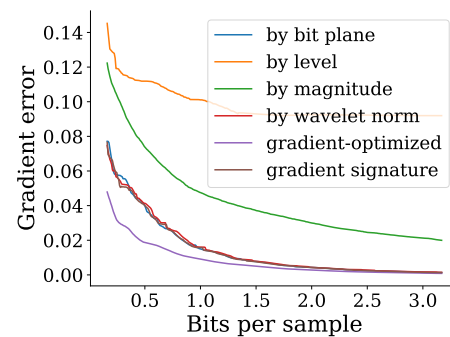
(l) vismale



(m) karfs



(n) aneurysm



(o) velocity z

Figure 3: Gradient using 5-point stencil

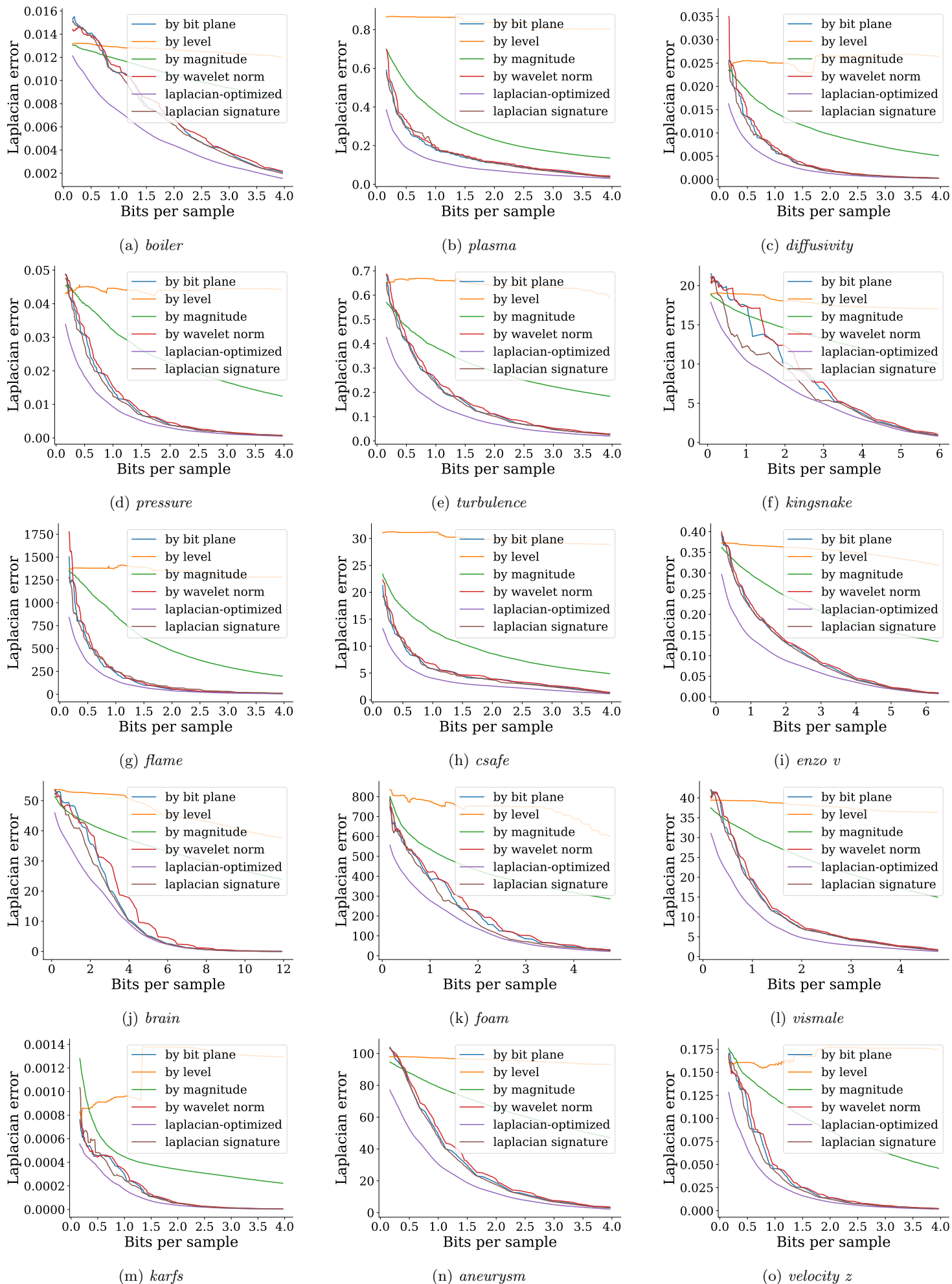


Figure 4: Laplacian using 5-point stencil

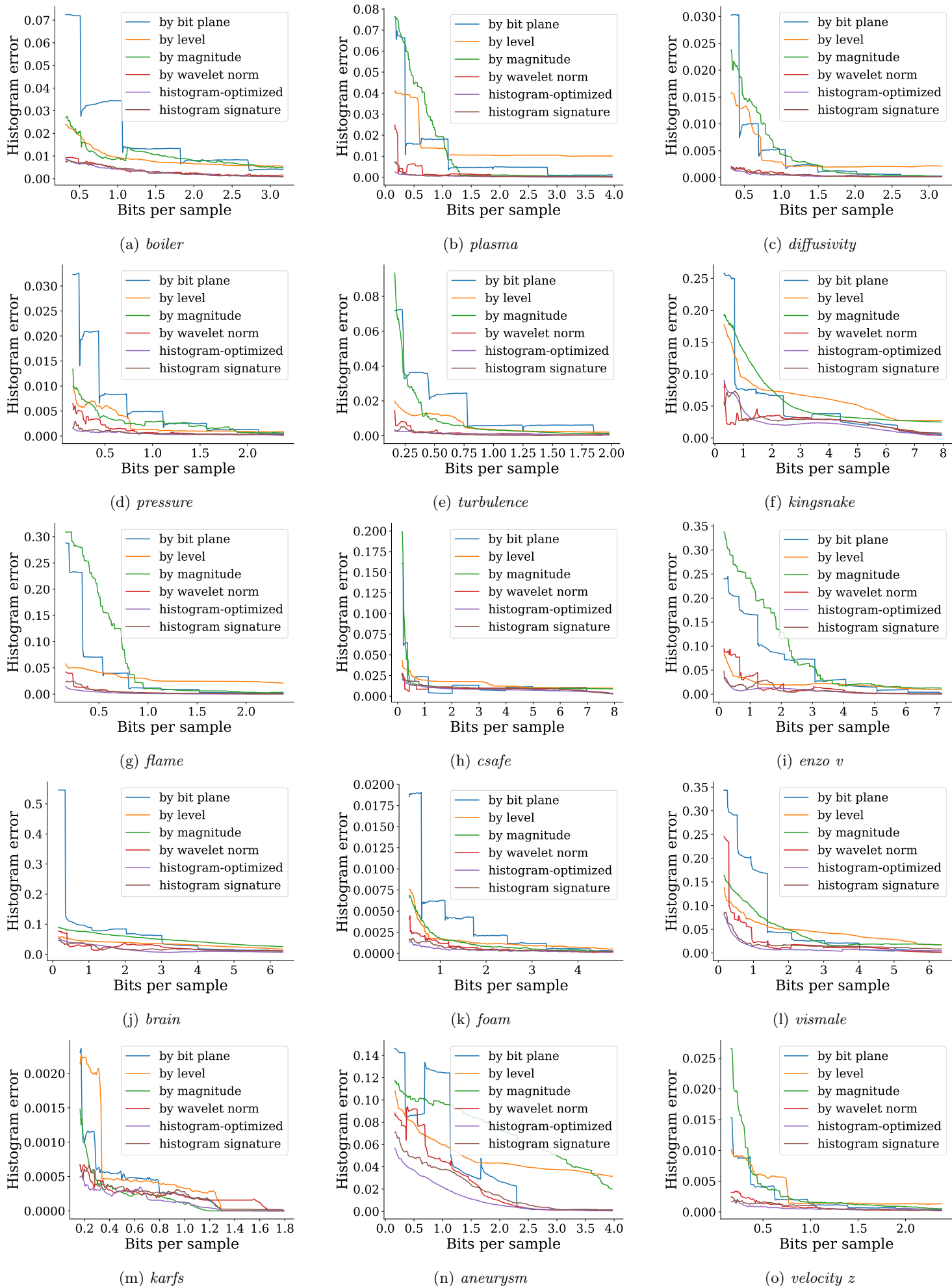
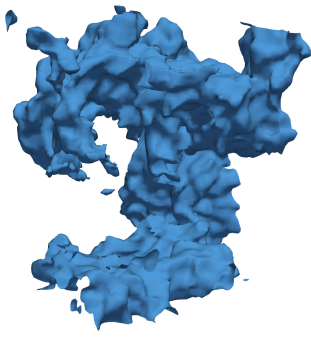


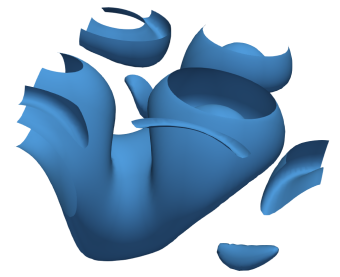
Figure 5: Histogram using 64 bins



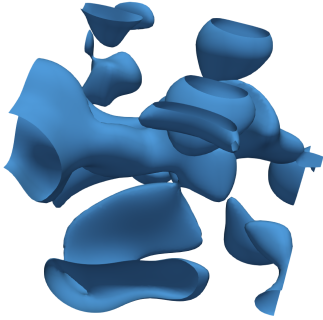
(a) boiler, isovalue=0.5



(b) plasma, isovalue=2



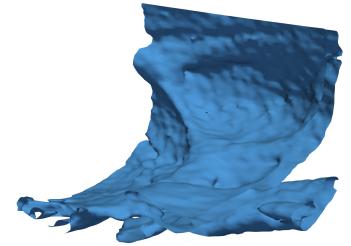
(c) diffusivity, isovalue=-0.05



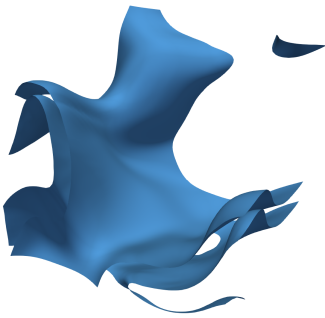
(d) pressure, isovalue=0.2



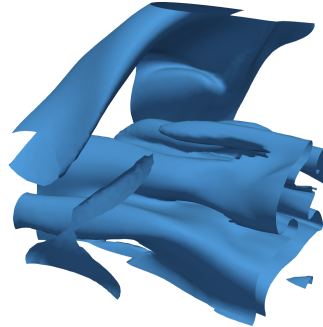
(e) turbulence isovalue=5



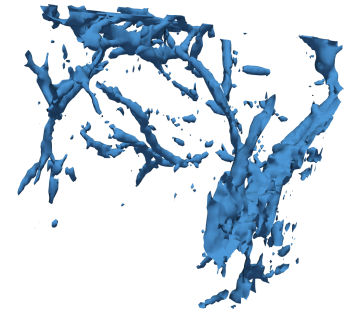
(f) kingsnake, isovalue=106



(g) flame, isovalue=-6000



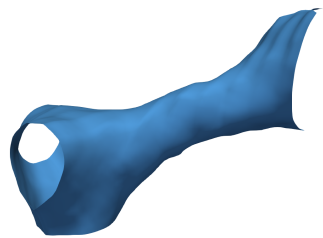
(h) csafe, isovalue=60



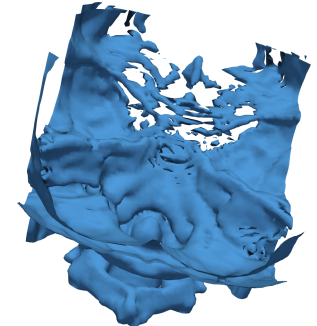
(i) enzo v isovalue=0.4



(j) brain, isovalue=90



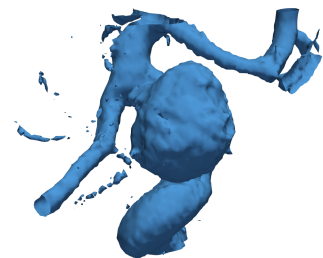
(k) foam, isovalue=30934



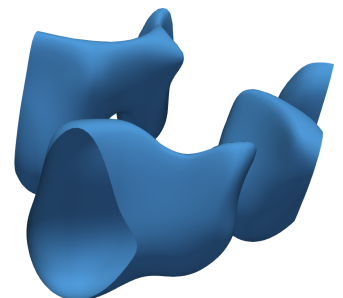
(l) vismale, isovalue=80



(m) karfs, isovalue=2.8



(n) aneurysm, isovalue=127



(o) velocity z, isovalue=-2

Figure 6: Isosurfaces (and isovalues) used for computing the isosurface errors

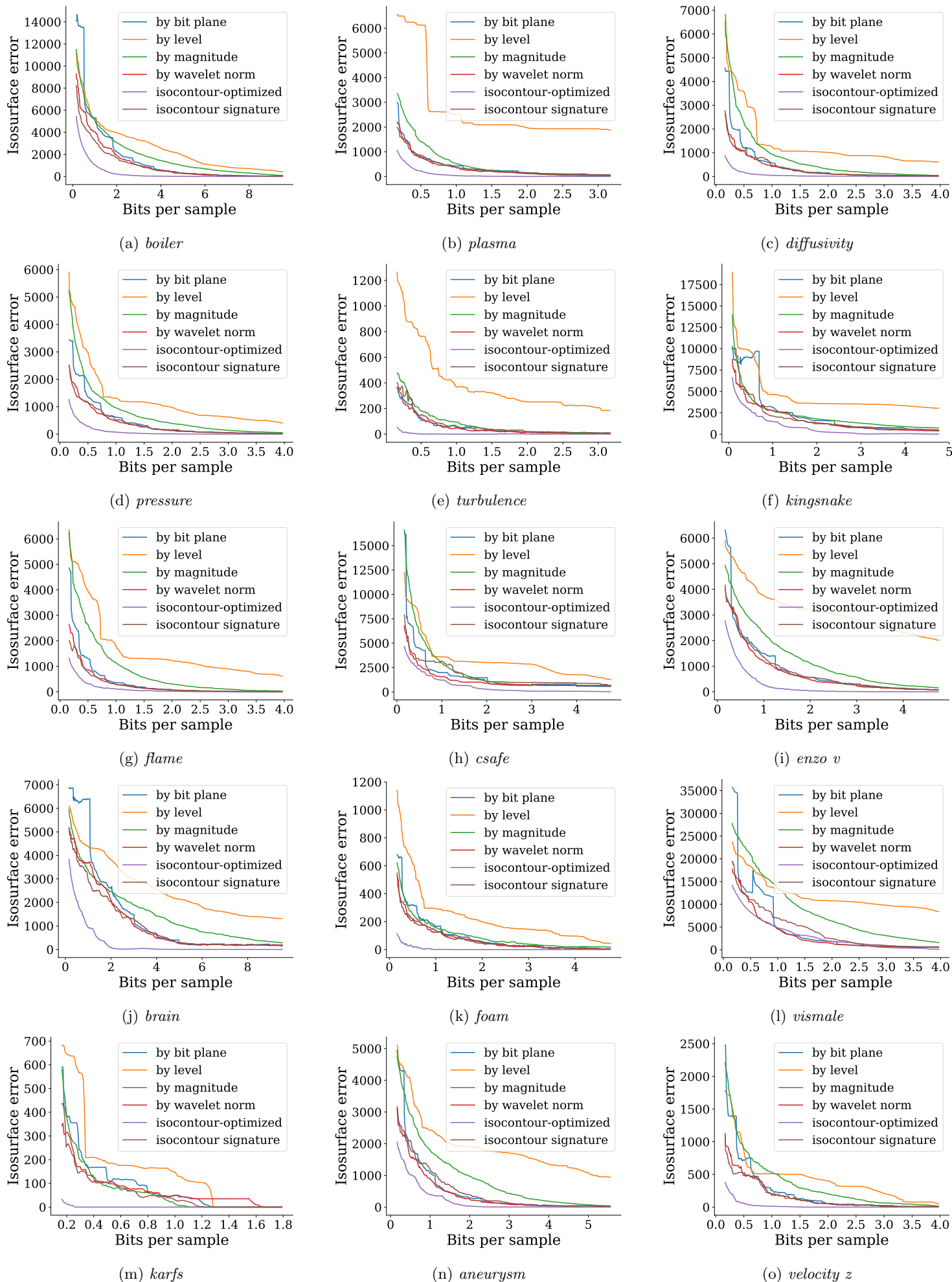


Figure 7: Isosurface